

# Preliminary Results of the Seismicity Monitoring Experiment around the 2019 *Mw*5.4 Earthquake Epicenter in the Central South China Sea Basin

Wenfei Gong<sup>1,2</sup>, Aiguo Ruan<sup>\*1,2,4</sup>, Xiongwei Niu<sup>2,5</sup>, Zhenjie Wang<sup>3</sup>, Pingchuan Tan<sup>2</sup>, Xiaodong Wei<sup>2</sup>, Wei Wang<sup>1,2</sup>, Zhengyi Tong<sup>2,4</sup>, Liqun Cheng<sup>2</sup>, Fansheng Kong<sup>2</sup>, Shaoping Lu<sup>5,6</sup>, Jianke Fan<sup>7</sup>, Weiwei Ding<sup>1,2,4</sup>, Jinyao Gao<sup>2</sup>, Chunguo Yang<sup>2</sup>, Jiabiao Li<sup>1,2,4</sup>

1. School of Oceanography, Shanghai Jiaotong University, Shanghai 200240, China

2. Key Laboratory of submarine Geosciences, Second Institute of Oceanography, Ministry of Natural Resources, Hangzhou 310012, China



3. Zhejiang Earthquake Administration, Hangzhou 310013, China


4. School of Earth Sciences, Zhejiang University, Hangzhou 310027, China

5. Southern Marine Science and Engineering Guangdong Laboratory (Zhuhai), Zhuhai 519082, China

6. School of Earth Sciences and Engineering, Sun Yat-sen University, Zhuhai 519082, China

7. Institute of Oceanology, Chinese Academy of Sciences, Qingdao 266071, China

 Wenfei Gong: <http://orcid.org/0000-0003-4133-1925>;  Aiguo Ruan: <http://orcid.org/0000-0003-4161-3789>;

 Xiongwei Niu: <https://orcid.org/0000-0003-1051-768X>

**ABSTRACT:** On September 5, 2019, a moderate earthquake of *Mw*5.4 unexpectedly occurred in the apparently quiescent central basin of the South China Sea. We immediately carried out a seismicity monitoring experiment around the epicenter by using broadband ocean bottom seismometers (OBS) for the following three scientific targets. The first is knowing the earthquake seismogenic mechanism, fault structure and further development. The second is finding the role of the residual spreading ridge playing in earthquake processes and further revealing the deep structures of the ridge directional turning area. The third is confirming the existence and significance of the so called “Zhongnan fault”. This paper reports the preliminary results of the first phase experiment. Five OBSs were deployed for seismicity monitoring with a duration of 288 days, but only three were recovered. Micro-earthquakes were firstly detected by an automatic seismic phase picking algorithm and then were verified by analyzing their seismic phases and time-frequency characteristics in detail. A total of 21, 68 and 89 micro-earthquakes were picked out from the three OBSs respectively within the distance of 30 km. The dominant frequency of these micro-earthquakes is 12–15 Hz, indicating tectonic fracturing. During the first two months after the mainshock the seismicity was relatively stronger, and micro-earthquakes were still occurring occasionally till the end of observation, indicating the epicenter area is active. We used Match&Locate method to locate 57 micro-earthquakes preliminarily. Their spatial distribution shows that the seismicity is developed mainly along the NE direction roughly parallel to the residual ridge with depth variations between 10–20 km.

**KEY WORDS:** South China Sea, microseismic monitoring, earthquakes, fault, broadband OBS.

## 0 INTRODUCTION

On September 5, 2019, a thrust-slide type earthquake of *Mw*5.4 occurred in the central basin of the South China Sea (SCS) (Fig. 1) with epicenter at longitude 116.16° E, latitude 14.77° N and focal depth of 20 km (China Earthquake Net-

works Center). It caused our concern and research interest because of the following considerations.

The focal mechanism of earthquakes occurred at the residual ridge may reflect some information of paleo spreading process, transform fault activity or magma activity (e.g., Stein and Klosko, 2002). If the 2019 *Mw*5.4 earthquake is confirmed to occur at the upper mantle of the SCS residual spreading ridge (crust thickness there is about 5–8 km, Ruan et al., 2016), it will make great changes about our knowledge of the SCS formation.

The SCS basin is a seismic quiescent area with few moderate earthquakes (Fig. 2) (Liu, 2002). The earthquakes concen-

\*Corresponding author: ruanag@163.com; xwniu@sio.org.cn

© China University of Geosciences (Wuhan) and Springer-Verlag GmbH Germany, Part of Springer Nature 2024

Manuscript received June 30, 2021.

Manuscript accepted December 24, 2021.

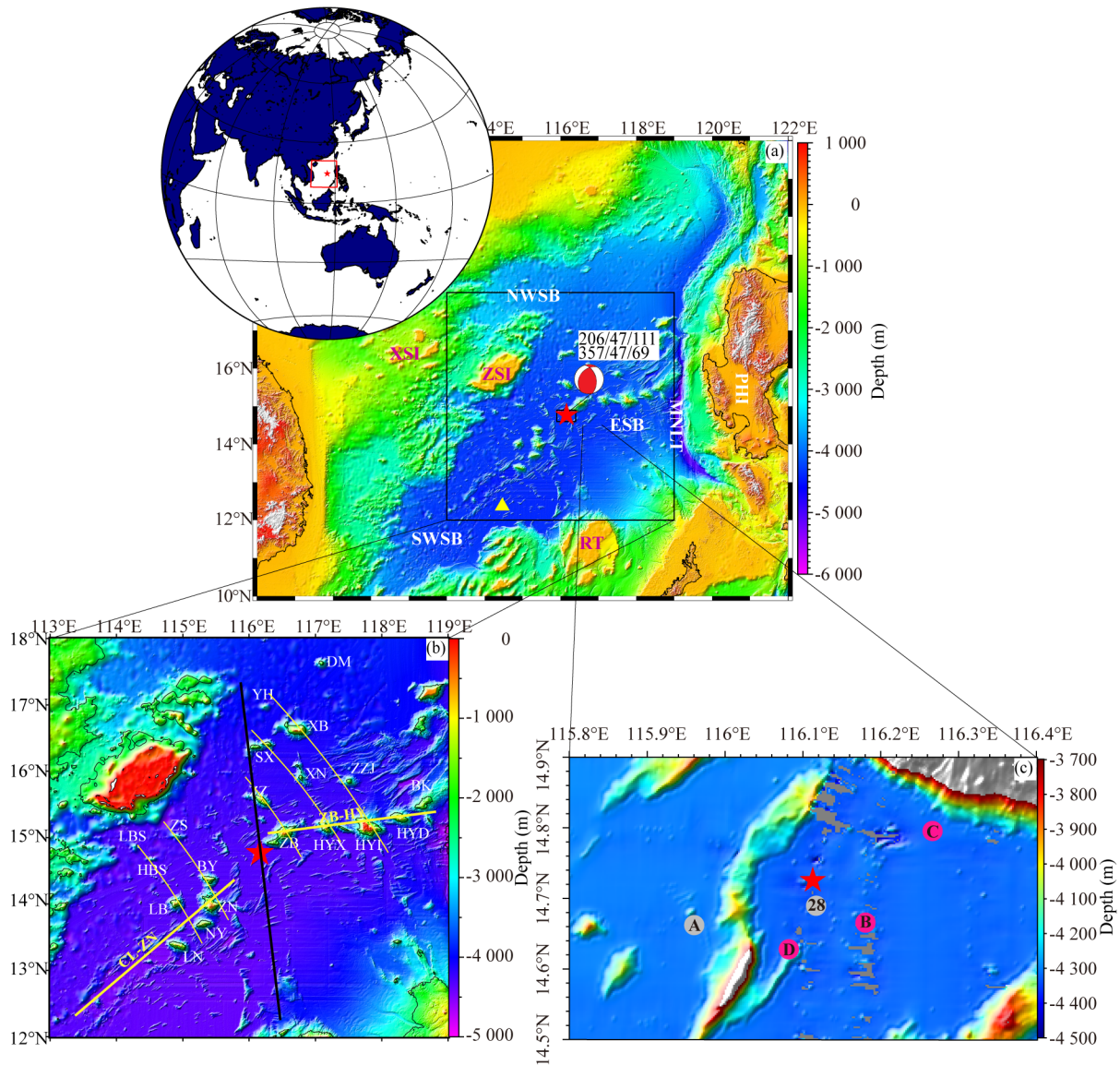


**Figure 1.** The geological setting of the research area and OBSs' locations of the seismicity monitoring experiment. (a) The geological setting of the research area with the location of the 2019 *Mw*5.4 earthquake (red star) and the 1965 *Ms*5.8 earthquake (yellow triangle). (b) The linear distribution of seamounts (white), the extension of spreading ridge (yellow) and “Zhongnan fault” (black). CL-ZN. “Changlong-Zhongnan” Seamount Chain; ZB-HY. “Zhenbei-Huangyan” Seamount Chain; LN. Longnan Seamount; NY. Nanyue Seamount; LB. Longbei Seamount; HBS. Hongbaoshi Seamount; LBS. Lanbaoshi Seamount; ZN. Zhongnan Seamount; BY. Beiyue Seamount; ZS. Zuanshi Seamount; ZB. Zhenbei Seamount; ZZJ. Zhangzhongjing Seamount; HYX. Huangyanxi Seamount; XN. Xiannan Seamount; SX. Shixing Seamount; YH. Yihang Seamount; XB. Xianbei Seamount; ZZJ. Zhangzhongjing Seamount; HYI. Huangyan Island; HYD. Huangyandong Seamount; BK. Beike Seamount; DM. Daimao Seamount. (c) The locations and terrains of the five OBSs; the topography data are multibeam data. NWSB. Northwestern sub-basin; ESB. Eastern sub-basin; SWSB. Southwestern sub-basin; XSI. Xisha Islands; ZSI. Zhongsha Islands; MNL. Manila Trench; PHI. Philippines; RT. Reed Bank.

trated in the Manila Trench and sporadically distributed in South China continental margin. The last moderate earthquake occurred 57 years ago on October 7, 1965 with magnitude of *Ms*5.8, epicenter at longitude 114.46°E, latitude 12.37°N and focal depth of 17 km (International Seismological Centre) beneath Southwestern sub-basin (SWSB) of the SCS (Fig. 1a). Due to lack of seismometers around the 1965 *Ms*5.8 earthquake, few studies have been done to reveal its seismogenic mechanism. According to the topography around the 1965 *Ms*5.8 earthquake, a normal fault may exist there (Wu and Wen, 2019), which may be the reason for the 1965 *Ms*5.8 earth-

quake. But because of an enormous distance (~324 km) between the 1965 *Ms*5.8 earthquake and the 2019 *Mw*5.4 earthquake, it is hard to conclude that there is a direct connection between them. Therefore, it is interesting to know the seismogenic mechanism, geological structure and subsequent development with time of this rare earthquake. It is also important to assess the impacts of the moderate mainshock and aftershocks on the seabed ecology and geological environment of the SCS central basin.

Seismicity of one area is a crucial window to study the crustal/mantle structure, stress field, fault characteristics and

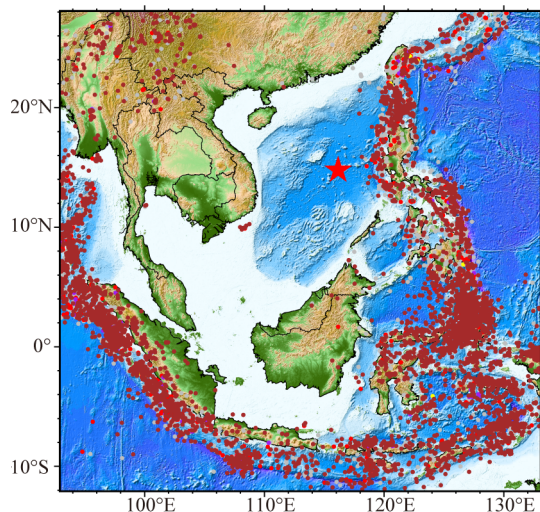


**Figure 2.** The distribution of earthquakes around the South China Sea. The red star represents the 2019  $M_w5.4$  earthquake.

magmatic activity in this area, especially for the seismic quiet area of sea basin where is no long-term seismic observation network. We noticed that the 2019  $M_w5.4$  earthquake occurred at the southern end of Zhenbei Seamount. The epicenter area is at the junction zone of “Changlong-Zhongnan” Seamount Chain with “Zhenbei-Huangyan” Seamount Chain where the residual spreading ridge changes its strike suddenly from NE in the SWSB to EW in the Eastern sub-basin (ESB). Also, the epicenter fell on the famous “Zhongnan fault” (Ruan et al., 2016; Barckhausen et al., 2014; Li and Song, 2012; Yao, 1994) (Fig. 1b).

After the 2019  $M_w5.4$  earthquake, we made a research plan including three phases of seismicity monitoring experiment in the SCS basin. The first phase of experiment was carried out immediately after the mainshock, and five broadband ocean bottom seismometers (OBS) were deployed around the mainshock epicenter (Fig. 1c). This paper reports the details of the first phase OBS experiment, the data and its processing and the preliminary analyzed results of the seismicity after the 2019  $M_w5.4$  earthquake.

## 1 SCIENTIFIC TARGETS OF THE SEISMICITY MONITORING EXPERIMENT

### 1.1 Seismogenic Mechanism of the 2019 $M_w5.4$ Earthquake and Subsequent Development

Due to the absence of seismic networks around the suddenly occurred earthquake, the published focal parameters that determined by remote land stations are not accurate enough. For example, the focal depth of the mainshock was suggested to be 20 km by China Earthquake Networks Center (CENC) or 11.2 km by United States Geological Survey (USGS). This is a crucial difference for an earthquake that occurred in the crust or in the mantle, because previous studies showed that the thickness of the SCS oceanic crust is only 5–8 km with water depth ~4 km (Ding et al., 2021; Zhao et al., 2018; Ruan et al., 2016; Qiu et al., 2011; Yao and Wang, 1983). Generally, the crust is relatively brittle and prone to earthquakes (Yu et al., 2018; Scholz, 2002). If a moderate earthquake occurs inside

the oceanic mantle, it might have very complicated mechanisms such as a remnant slab removal fractured caused by large-scale mantle magmatism beneath the residual spreading ridge and fractured (Wang et al., 2016) or lithospheric local convection and destruction due to subducted plate rollback (Fan and Zhao, 2021; Niu, 2013). Monitoring on micro-earthquakes spatial distribution would reveal the focal depth and seismogenic fault (Ha et al., 2022). Moreover, although it is impossible to obtain this earthquake precursory, we are strongly interested in knowing its type and further development through the monitoring experiment. Because the impacts of the seismic activities on the seabed environment at the epicenter area are also of global interest. Moreover, the micro-seismic activities and their development trend after the mainshock are also the basis for studying other related scientific targets.

### 1.2 Deep Structure of the Residual Spreading Ridge of the SCS

The spatial distribution of seamounts in the SCS basin has distinguished linear structural characteristics (Fig. 1b, white solid line), especially the seamount chains of the residual ridge extending from the SWSB to the Manila trench at the eastern border. And the residual spreading ridge changes its strike direction between “Changlong-Zhongnan” Seamount Chain and the “Zhenbei-Huangyan” Seamount Chain (Li and Song, 2012; Briaies et al., 1993). It is interesting that the 2019  $M_w5.4$  earthquake is just located in the area where the residual spreading ridge strike changes abruptly and its one mechanism solution of faulting strike is  $206^\circ$  roughly parallel to that of “Changlong-Zhongnan” Seamount Chain in the SWSB. However, its deep mechanism is still unclear. We noticed that the profile OBS2014-ZN roughly crosses the  $M_w5.4$  epicenter area (Ruan et al., 2016) and its velocity anomaly model reveals that the epicenter of the 2019  $M_w5.4$  earthquake is approximately at the junction of high-speed anomaly and low-speed anomaly. Therefore, the observation of micro seismicity around the epicenter area together with remote earthquakes might help us understand the residual spreading ridge deep structure and its role in the SCS formation mechanism and evolution.

### 1.3 “Zhongnan Fault” Structure Dynamics and Its Role in the SCS Evolution

We also noticed that one mechanism solution of the mainshock faulting strike is  $357^\circ$  roughly parallel to that of “Zhongnan fault” and the epicenter is also just on the fault. This large-scale fault is thought to be a deeply fractured system with NW strike and passing through the whole SCS and separating the basin into two parts (Xu et al., 2021; Ruan et al., 2016; Barckhausen et al., 2014; Li and Song, 2012; Yao, 1995). Huang et al. (2019) recently put forward a new hypothesis for the SCS in which the “Zhongnan fault” plays an important shear striking role in opening up the SCS. Through seismicity monitoring, we could find out deep dynamic mechanism, focal depth and fault dislocating strike of the mainshock which can help us understand whether it is related to “Zhongnan fault” or not. In other words, due to the particular position of the experiment, the monitoring data also provide possibilities to understand



“Zhongnan fault” dynamics, its relationship with the residual spreading ridge and its role in the evolution of the SCS.

## 2 SEISMICITY MONITORING EXPERIMENT AROUND THE 2019 *Mw*5.4 EARTHQUAKE EPICENTER AREA (PHASE I)

After the 2019 *Mw*5.4 earthquake occurred in the SCS central basin, we immediately carried out a seismicity monitoring experiment around the epicenter by using broadband ocean bottom seismometers (OBS). We also designed an experiment plan of three consecutive monitoring phases: October 2019 to July 2020, July 2020 to May 2021 and May 2021 to May 2022. The OBSs used in the seismicity monitoring experiment are developed by Institute of Geology and Geophysics, Chinese Academy of Sciences which are all composed of three geophones and one hydrophone with a frequency of 30 s-150 Hz and a sampling rate of 50 Hz. This paper reports the first phase of the experiment and its preliminary results.

The OBS deployment cruise for the first experiment phase was conducted from October 5, 2019 to October 6, 2019 by using a fishing boat named “Lurong·Yuanyuyun 899”, and deployed five OBSs around the mainshock epicenter with a minimum distance of ~3 km and a maximum distance of ~15 km. The coordinates of OBS stations are listed in Table 1. From July 18, 2020 to July 19, 2020, we recovered the OBSs by using the same fishing boat. Three OBSs (B, C, D) were recovered but two were lost. GPS was used for timing (UTC) and positioning. The maximum recording time of recovered OBSs is 288 days, and the minimum is 81 days. See Table 1 for details.

### 2.1 Data Processing

The data were processed as follows: (1) Converting the raw data format into the general used sac format; (2) Using linear method to correct the clock drift time after time calibration by GPS; (3) Inputting the various information of OBS stations into the header files, respectively; (4) Using a band-pass filter of 1–15 Hz to reduce the interference of noise to micro signals.

### 2.2 Automatic Selection of Micro-Seismic Events

The method combined the ratio of Short-Term Average energy to Long-Term Average energy (STA/LTA) with Auto Regression Akaike Information Criterion (AR-AIC) (Sleeman and van Eck, 1999) is adopted to automatically detect the micro-seismic events and pick up phase arrival time. The operation processes are as follows: First, a new time series called characteristic function (CF) is constructed to replace the original seis-

mic signal. It can sensitively respond to the change in signal frequency or amplitude. Then, we select classic STA/LTA and calculate energy content attribute of two different length of time windows, a short-term average (generally 1–2 s) and a long-term average (generally 10s). The amplitude of signal change is enhanced by calculating the ratio of STA/LTA. Next, the advent of the given phase is estimated by a setting threshold of CF value. Finally, we precise arrival time of seismic phases through utilizing Auto-Regressive (AR) model and Akaike Information Criterion (AIC) as described to determine. The minimum AIC value which corresponding time-point is the P (or S) arrival time. Figure 3 shows the waves arrivals picking out method and results of one micro-seismic event. The summary of the picked out micro-seismic events from the three OBSs is listed in Table 1. Among them, there are 21 micro-seismic events recorded by all three OBSs at the same time and 45 ones recorded by two OBSs.

### 2.3 Verification of the Selected Micro-Earthquakes

In order to confirm the picked out micro-earthquakes and to affirm accurately the time of waves arrivals, we calculated short-time Fourier transforms with a 1-s (i.e., 50 samples) sliding window, Hanning tapering and an overlap of 45 samples to analyze the time-frequency characteristics of micro-earthquakes. Figure 3 shows one OBS four components filtered waveforms and spectra of one micro-earthquake as an example. It is analyzed as follows.

(1) The direct P-wave and S-wave phases are clearly recorded in OBS three components. The hydrophone component that has no S-wave signal is useful in highlight of both P-wave and S-wave arrivals in OBS three components.

(2) According to the automatically picked out P-wave arrival, we can roughly estimate the distance of this micro-earthquake relative to Station B about 24.9 km, by supposing  $V_p$  6.0 km/s and  $V_s$  3.5 km/s.

(3) In addition, based on waveforms and their spectra, we manually identified that the arrivals of P-wave and S-wave are nearly the same as the automatically picked out. Therefore, we always used automatic method to pick out micro-seismic events first and then manually to re-determine their accurate wave arrivals again.

(4) According to the energy spectra, the dominant frequencies are 12–15 Hz for P-wave and 6–9 Hz for S wave, respectively. It indicates that the micro-earthquake is of tectonic rupturing (Konstantinou et al., 2013).

(5) Both the waveform and spectrum of hydrophone com-

**Table 1** OBS coordinate, record duration, epicenter distance and result of picking out micro-earthquakes in Phase I

Number	Origin/deployed time (UTC)	Recovered time (UTC)	Lon. (°)	Lat. (°)	Epicentral distance (km)	Depth (km/m)	Recovery	Record duration (d)	Micro-earthquake number
<i>Mw</i> 5.4	2019.09.05 13:58:35	-	116.160 0	14.770 0	-	20	-	-	-
28	2019.10.05 07:31:14	-	116.163 6	14.742 7	3.045	4 300	×	-	-
A	2019.10.05 08:37:41	-	116.032 4	14.721 8	14.738	4 286	×	-	-
B	2019.10.06 07:04:33	2020.07.19 01:09:30	116.216 7	14.724 6	7.906	4 300	√	81	68
C	2019.10.05 06:15:33	2020.07.18 22:45:00	116.289 1	14.823 0	15.084	4 300	√	288	21
D	2019.10.05 07:58:24	2020.07.19 03:30:00	116.134 2	14.695 8	8.667	4 251	√	288	89

The hypocenter parameters are based on ISC; Lon. Longitude; Lat. Latitude.

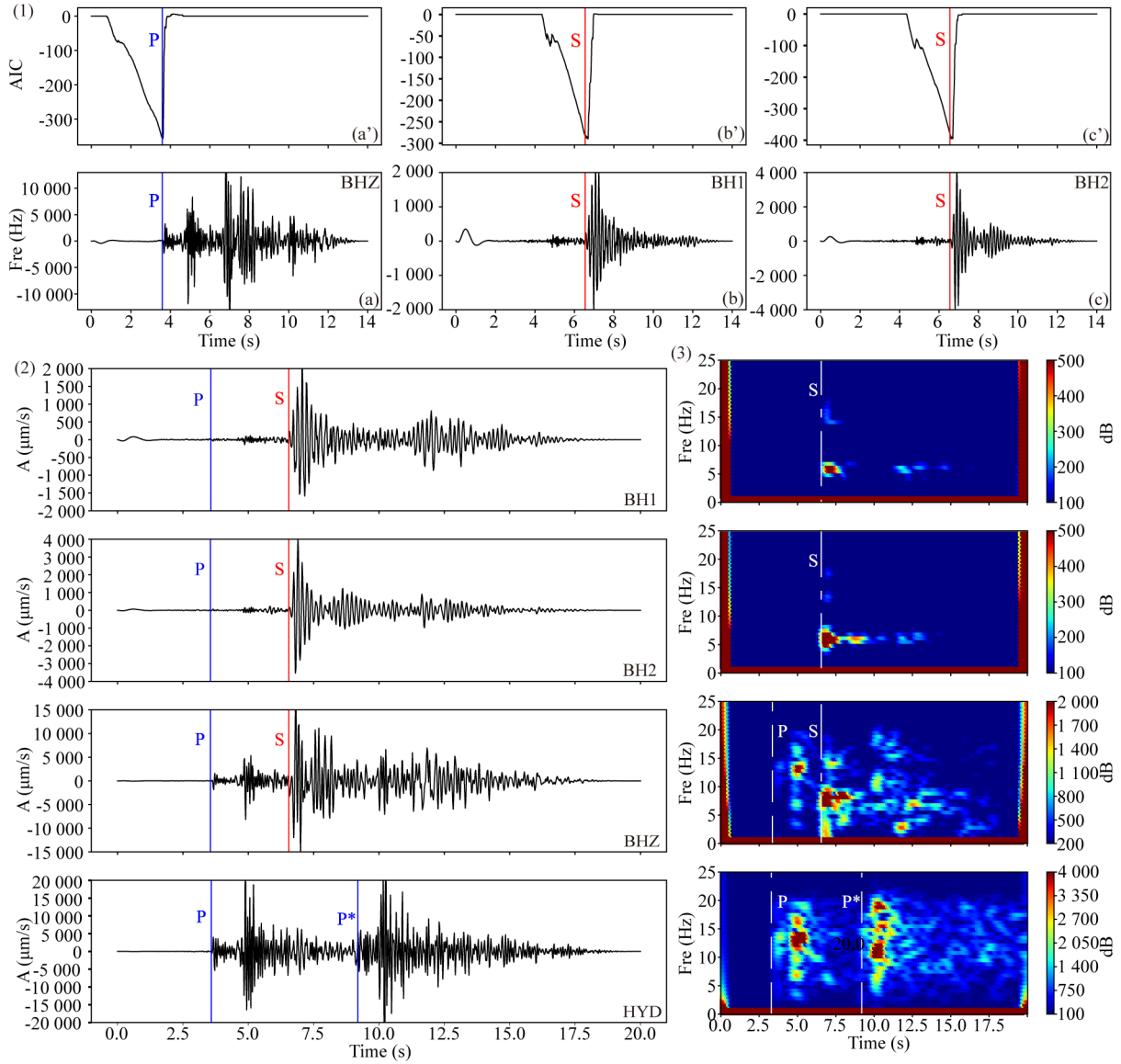


**Figure 3.** The method for picking out one micro-seismic event of Station B. (1) The automatic method combined STA/LTA with AR-AIC. In this case, the arrival time of P wave is 3.59 s and S wave is 6.55 s. (2) The further manually identification of micro-earthquake in waveforms. (3) The analysis of waveform spectra of the micro-earthquake.

ponent show that, in addition to the direct P-wave, the secondary P-wave phase reflected by water surface is also recorded. The interval between the direct wave and the secondary wave is about 5.5 s, which is consistent with the water depth of 4 300 m (velocity is  $\sim 1.5$  km/s).

#### 2.4 The Seismicity after the 2019 *Mw*5.4 Earthquake

One of the most important targets of this seismicity monitoring experiment in the SCS basin is to trace seismic activity development after the 2019 *Mw*5.4 earthquake. We counted the number of the picked out micro-earthquakes from three OBS stations respectively with 7 days as a statistics unit and plot them in Fig. 4.

(1) After the mainshock, from the very beginning to November 1 (56 days), the micro seismicity around the epicenter area was remarkable with the maximum frequency of 6 times/day. It was then followed by a downward tendency but it did

not stop thoroughly.

(2) The number of micro-earthquakes recorded by Station B in October 2019 was obviously larger than that of the other two stations. In contrast, Station C recorded very fewer, only 1–2 times a week. Except the difference in effective observation time among three OBSs due to equipment technique problems such as water leakage (which resulted in two OBSs were failed to be recovered), we think the distances or seafloor geographies between stations and the micro-earthquake epicenters maybe the important factors for observation efficiency. For instance, Station B recorded a high frequency of micro-earthquakes at the very beginning because of its small distance and flat terrain, but failed to record anymore after 81 days due to its equipment problem. In contrast, although Station C had been working normally, its recording efficiency is not good enough because of its farther distance ( $\sim 15$  km) and the obstruction of seamount.

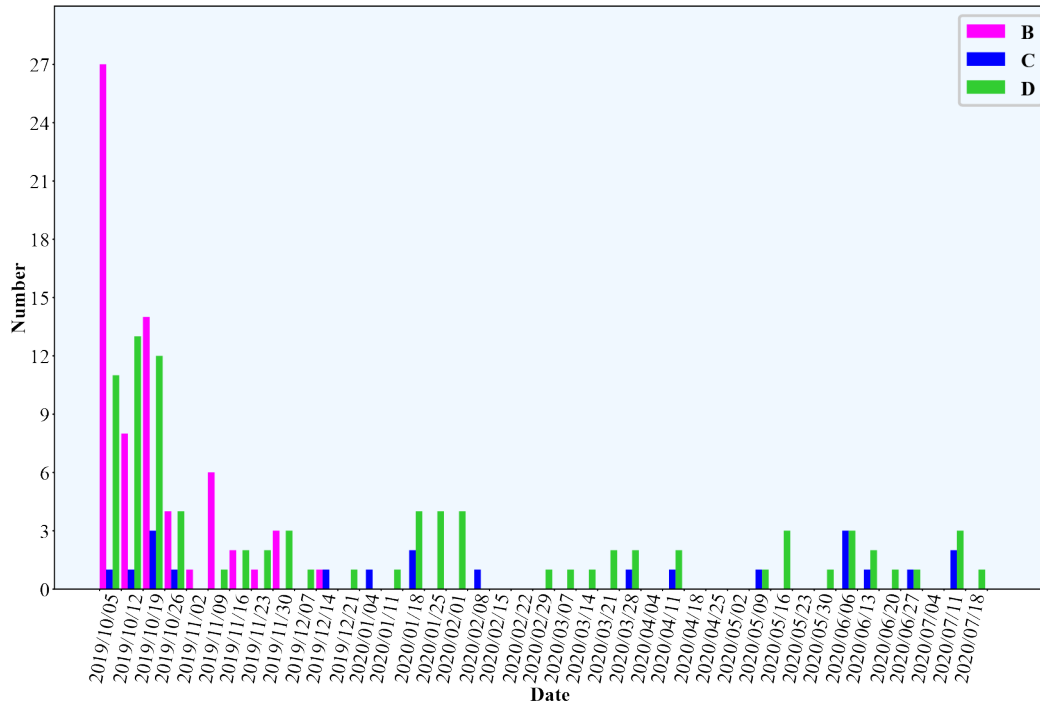


Figure 4. Seismicity development after the 2019 *Mw*5.4 earthquake. Picking out micro-earthquakes with 7 days as a statistics unit.

(3) According to the gradually reduced seismicity frequency in the experiment area, we think after the 2019 *Mw*5.4 earthquake, the influence of micro-earthquakes on seabed environment is limited.

## 2.5 Locating Micro-Earthquakes with Match & Locate Method

Match & Locate (M&L) (Zhang and Wen, 2015) method is more sensitive to weak seismic signals and less dependent on velocity models. It can detect and locate micro-earthquakes with lower magnitude and poor signal-to-noise ratio. Its operation processes are as follows: (1) Selecting an event of clear seismic phases and high signal-to-noise ratio as a template event (Fig. 5) and determining its location. (2) Calculating slide cross-correlation function between template reference phase waveforms (e.g., S phase) and all continuous waveforms recorded by three OBSs. At the same time, three-dimensional meshing in longitude, latitude and depth is applied to the area taking the template event as center (e.g., search scope:  $0.15^\circ/0.15^\circ/10$  km; search accuracy:  $0.01^\circ/0.01^\circ/2$  km), and calculating travel time differences between the template location and each grid point. (3) Stacking the cross-correlation waveforms based on the corresponding travel time differences and calculating mean correlation coefficient (mean CC) and signal-to-noise ratio. (4) Determining the location of the detected event at the grid point with the maximum mean CC when they exceed the pre-set threshold (e.g., 0.3/12).

In this study, Station B stopped recording on December 25, 2019, while M&L method needs at least three stations, therefore, only 57 micro-earthquakes (Table S1) occurred from October 5, 2019 to December 25, 2019 were preliminarily located. The spatial distribution of 57 micro-earthquakes (Fig. 6) shows that the seismicity is developed in a large area mainly

along the NE direction roughly parallel to the residual ridge with some diversities. Their depth variations suggest that the seismogenic zone is large, and it is difficult to confirm accurately the main shock depth at present.

## 3 CONCLUSIONS

This paper introduces the first phase of seismicity monitoring experiment in the SCS basin around the epicenter area of the 2019 *Mw*5.4 earthquake, and presents some preliminary results.

### 3.1 The Seismicity after the 2019 *Mw*5.4 Earthquake

After the 2019 *Mw*5.4 earthquake, there are indeed some micro-earthquakes occurred around the epicenter. Their time development shows that the closer to the 2019 *Mw*5.4 earthquake, the higher occurrence frequency of micro-earthquakes. The seismicity downward trend suggests the 2019 *Mw*5.4 earthquake is of mainshock-aftershocks type with lasting time at least 8 months or more. But according to their reducing tendency with time, we think their influence on the seabed is limited. The waveform spectra indicate that the observed micro-earthquakes are tectonic ones with a dominant frequency of 12–15 Hz, not caused by magmatic activities.

### 3.2 Relationship between the 2019 *Mw*5.4 Earthquake and the Residual Spreading Ridge or “Zhongnan Fault”

The preliminary positioning results show that the seismicity after the mainshock is developed in a large area mainly along the NE direction roughly parallel to the residual ridge with some diversities. This is a result of very important significance which suggests the residual ridge is still active and responsible for the mainshock. In other words, “Zhongnan fault” has no relation with the 2019 *Mw*5.4 earthquake. We believe

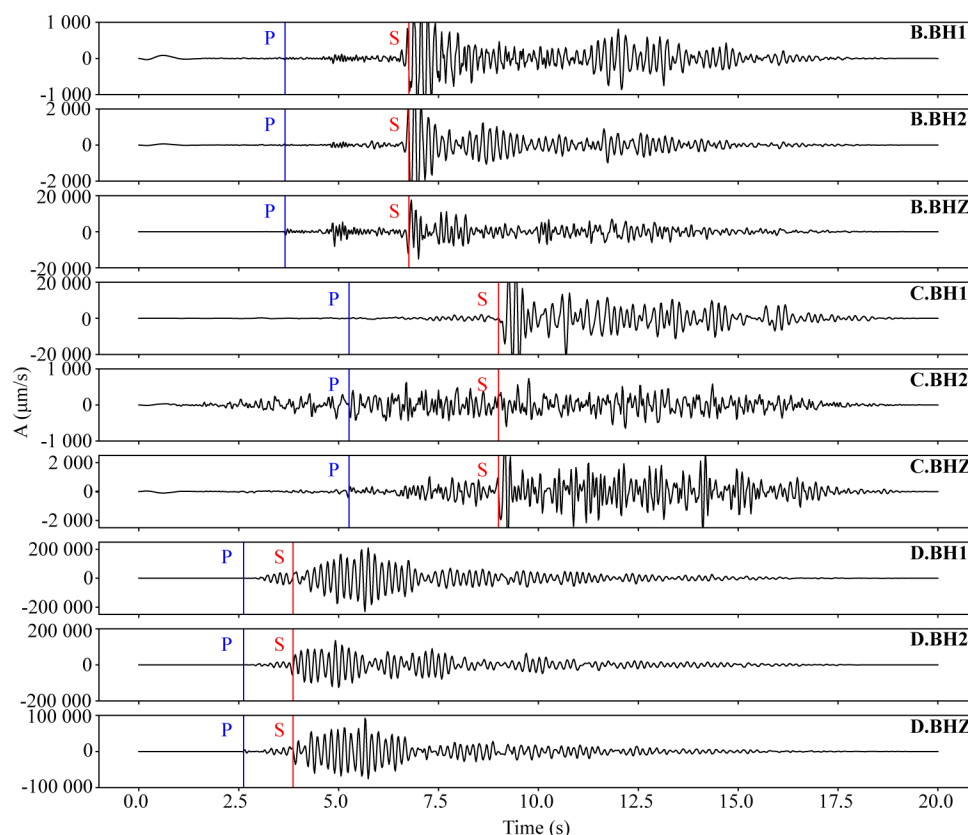


**Figure 5.** A template micro-seismic event recorded by three OBSs for Match & Locate method. The reference time is the seismogenic time (UTC): 09:24:30.36 on October 11, 2019.

these micro-earthquakes spatial distribution is beneficial to reveal the spreading ridge deep structure through future detailed study.

### 3.3 About the Mainshock Focal Depth

In this study, the depths of most micro-earthquakes are located from 10 to 20 km suggest there is a larger seismogenic area. It should explain why USGS and CENC gave so obviously different focal depths. However, at present we cannot give out an accurate focal depth either. In the further study, we will try new method to accurately locate micro-earthquakes and combine the constraints from deep lithosphere structure to determine focal depth of the 2019 *M*<sub>w</sub>5.4 earthquake.

### 3.4 Prospect

The seismicity monitoring experiment around the 2019 *M*<sub>w</sub>5.4 earthquake epicenter area is proceeding as planned. At present, it is in the process of OBS recovery of the second phase from July 2020 to May 2021 and OBS deployment of the third phase from May 2021 to May 2022. Therefore, more data are expectable. The future researches mainly include three aspects as follows.

(1) Based on previous active seismic profiles and tomography results in the study area, we will construct 3-D velocity models to relocate hypocenter of the picked micro-earthquakes and reveal *M*<sub>w</sub>5.4 earthquake faulting mechanism and focal depth.

(2) To further understand the geological background of

the SCS seismicity, remote earthquakes recordings are about to be used to study velocity structure of lithosphere, the thickness of mantle transition zone and the direction of mantle flow by using tele-seismic receiver function and anisotropy methods.

(3) Combined the two study aspects mentioned above with numerical simulation, we can analyze some more complicated questions related to the residual ridge or to “Zhongnan fault”, especially the question of their roles in the SCS evolution process.

### ACKNOWLEDGMENTS

This work was jointly supported by the National Natural Science Foundation of China (Nos. 42076047, 41890811). Some figures were prepared with GMT public domain software (Wessel and Smith, 1995). We thank all the scientists and crew who have participated in the South China Sea 2019 and 2020 OBS expeditions. The final publication is available at Springer via <https://doi.org/10.1007/s12583-021-1604-y>.

**Electronic Supplementary Materials:** Supplementary material (Table S1) is available in the online version of this article at <https://doi.org/10.1007/s12583-021-1604-y>.

### Conflict of Interest

The authors declare that they have no conflict of interest.

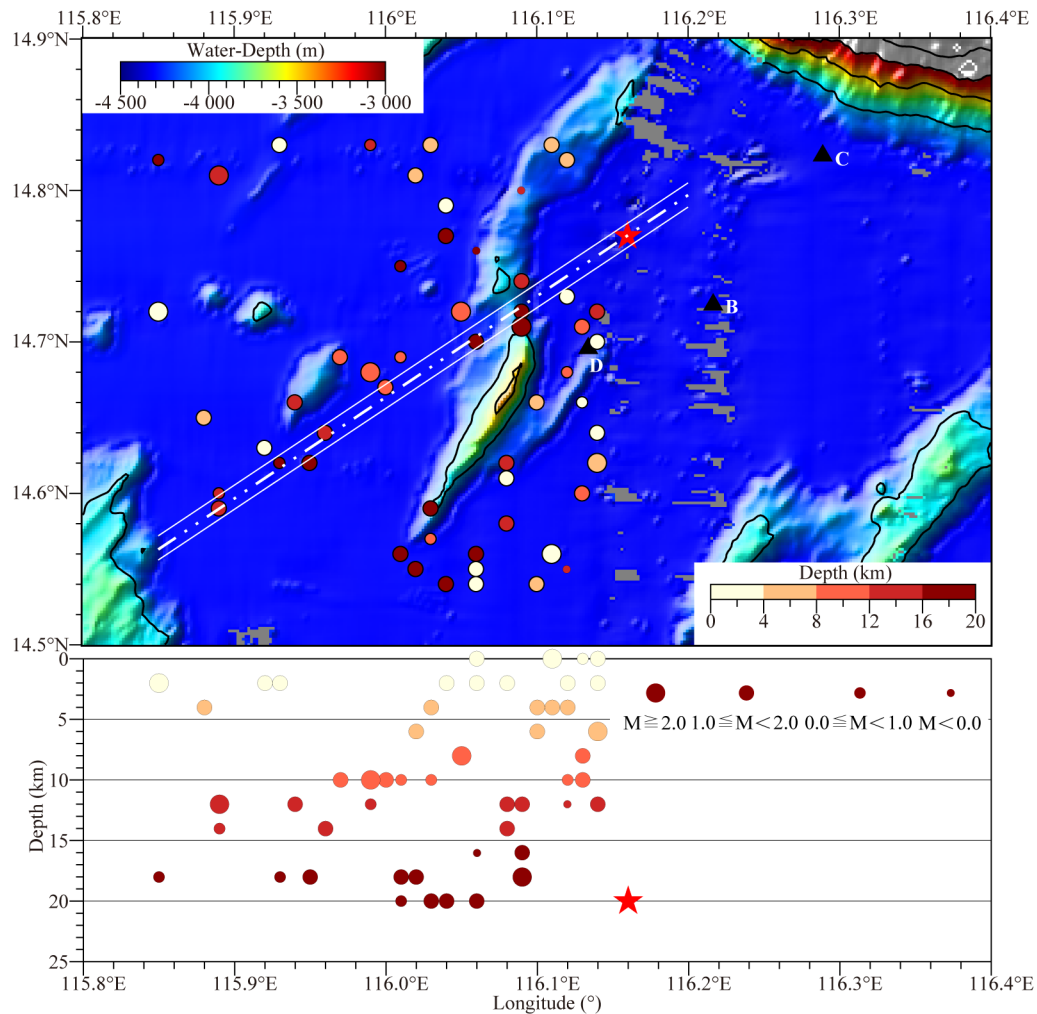


**Figure 6.** Spatial distribution of 57 micro-earthquakes and mainshock with the 2019 *M*<sub>w</sub>5.4 earthquake. The red star represents the 2019 *M*<sub>w</sub>5.4 earthquake. The black triangle represents the location of three OBSs. The color represents the focal depth. The darker the color, the greater the depth. The size of the circle represents the magnitude. The larger the circle, the greater the magnitude.

#### REFERENCES CITED

- Barckhausen, U., Engels, M., Franke, D. et al., 2014. Evolution of the South China Sea: Revised Ages for Breakup and Seafloor Spreading. *Marine and Petroleum Geology*, 58: 599–611. <https://doi.org/10.1016/j.marpetgeo.2014.02.022>
- Briaux, A., Patriat, P., Tapponnier, P., 1993. Updated Interpretation of Magnetic Anomalies and Seafloor Spreading Stages in the South China Sea: Implications for the Tertiary Tectonics of Southeast Asia. *Journal of Geophysical Research: Solid Earth*, 98(B4): 6299–6328. <https://doi.org/10.1029/92jb02280>
- Ding, H. H., Ding, W. W., Zhang, F., et al., 2021. Asymmetric Deep Structure of the South China Sea Basin and Its Controlling Factors. *Earth Science*, 46(3): 929–941. <https://doi.org/10.3799/dqkx.2020.338> (in Chinese with English Abstract)
- Fan, J. K., Zhao, D. P., 2021. P-Wave Tomography and Azimuthal Anisotropy of the Manila-Taiwan-Southern Ryukyu Region. *Tectonics*, 40(2): e2020TC006262. <https://doi.org/10.1029/2020TC006262>
- Ha, G. H., Liu, J. R., Ren, Z. K., et al., 2022. The Interpretation of Seismogenic Fault of the Maduo *M*<sub>w</sub> 7.3 Earthquake, Qinghai Based on Remote Sensing Images—A Branch of the East Kunlun Fault System. *Journal of Earth Science*, 33(4): 857–868. <https://doi.org/10.1007/s12583-021-1556-2>
- Huang, C. Y., Wang, P. X., Yu, M. M. et al., 2019. Potential Role of Strike-Slip Faults in Opening up the South China Sea. *National Science Review*, 6(5): 891–901. <https://doi.org/10.1093/nsr/nwz119>
- Konstantinou, K. I., Pan, C. Y., Lin, C. H., 2013. Microearthquake Activity around Kueishantao Island, Offshore Northeastern Taiwan: Insights into the Volcano-Tectonic Interactions at the Tip of the Southern Okinawa Trough. *Tectonophysics*, 593: 20–32. <https://doi.org/10.1016/j.tecto.2013.02.019>
- Li, C. F., Song, T. R., 2012. Magnetic Recording of the Cenozoic Oceanic Crustal Accretion and Evolution of the South China Sea Basin. *Chinese Science Bulletin*, 57(20): 1879–1895 (in Chinese)
- Liu, Z. S., 2002. *Geology of the South China Sea*: 1st Ed. Science Press, Beijing (in Chinese)
- Niu, Y. L., 2013. *Global Tectonics and Geodynamics: A Petrological and Geochemical Approach*. Science Press, Beijing (in Chinese)
- Qiu, X. L., Zhao, M. H., Ao, W. et al., 2011. OBS Survey and Crustal Structure of the Southwest Sub-Basin and Nansha Block, South China Sea. *Chinese Journal of Geophysics*, 54(12): 3117–3128 (in Chinese with English Abstract)
- Ruan, A. G., Wei, X. D., Niu, X. W. et al., 2016. Crustal Structure and Fracture Zone in the Central Basin of the South China Sea from Wide Angle Seismic Experiments Using OBS. *Tectonophysics*, 688: 1–10.



- <https://doi.org/10.1016/j.tecto.2016.09.022>
- Scholz, C. H., 2002. *The Mechanics of Earthquakes and Faulting*. Cambridge University Press, Cambridge. <https://doi.org/10.1017/cbo9780511818516>
- Sleeman, R., van Eck, T., 1999. Robust Automatic P-Phase Picking: An On-Line Implementation in the Analysis of Broadband Seismogram Recordings. *Physics of the Earth and Planetary Interiors*, 113(1/2/3/4): 265–275. [https://doi.org/10.1016/S0031-9201\(99\)00007-2](https://doi.org/10.1016/S0031-9201(99)00007-2)
- Stein, S., Klosko, E., 2002. *Earthquake Mechanisms and Plate Tectonics*. *International Geophysics*. Elsevier, Amsterdam. 69–78. [https://doi.org/10.1016/s0074-6142\(02\)80210-8](https://doi.org/10.1016/s0074-6142(02)80210-8)
- Wang, X. Y., Zhao, D. P., Li, J. B., 2016. The 2013 Wyoming Upper Mantle Earthquakes: Tomography and Tectonic Implications. *Journal of Geophysical Research: Solid Earth*, 121(9): 6797–6808. <https://doi.org/10.1002/2016jb013118>
- Wessel, P., Smith, W. H. F., 1995. New Version of the Generic Mapping Tools. *Eos, Transactions American Geophysical Union*, 76(33): 329. <https://doi.org/10.1029/95eo00198>
- Wu, Z. Y., Wen, Z. H., 2019. *Map Series of Marine Geology of China Seas*. Science Press, Beijing (in Chinese)
- Xu, Z. Y., Wang, J., Yao, Y. J., et al., 2021. The Temporal-Spatial Distribution and Deep Structure of the Zhongnan- Liyue Fault Zone in the North of the South China Sea Basin. *Earth Science*, 46(3): 942–955 (in Chinese with English Abstract)
- Yao, B. C., 1995. Characteristics and Tectonic Meaning of Zhongnan-Liyue Fault. *Geological Research of South China Sea*, 7: 1–14 (in Chinese)
- Yao, B. C., Wang, G. Y., 1983. Crustal Structure of the South China Sea Basin. *Science in China, Ser B*, 26(6): 648–661
- Yao, B. C., Zeng, W. J., Hayes, D. E., 1994. Research Report on China United States Cooperative Research on the Geology of the South China Sea. China University of Geosciences Press, Wuhan (in Chinese with English Abstract)
- Yu, Z. T., Li, J. B., Niu, X. W. et al., 2018. Lithospheric Structure and Tectonic Processes Constrained by Microearthquake Activity at the Central Ultraslow-Spreading Southwest Indian Ridge (49.2° to 50.8° E). *Journal of Geophysical Research: Solid Earth*, 123(8): 6247–6262. <https://doi.org/10.1029/2017jb015367>
- Zhang, M., Wen, L. X., 2015. An Effective Method for Small Event Detection: Match and Locate (M&L). *Geophysical Journal International*, 200(3): 1523–1537. <https://doi.org/10.1093/gji/ggu466>
- Zhao, M. H., He, E. Y., Sibuet, J.-C., et al., 2018. Postseafloor Spreading Volcanism in the Central East South China Sea and Its Formation through an Extremely Thin Oceanic Crust. *Geochemistry*, 19(3): 621–641. <https://doi.org/10.1002/2017GC007034>